1995 IEEE INTERNATIONAL FREQUENCY CONTROL SYMPOSIUM

Systematic Errors in Cesium Beam Frequency Standards Introduced by Digital Control of the Microwave Excitation

W. D. Lee, J. H. Shirley, F. L. Walls, and R. E. Drullinger
National Institute of Standards and Technology
Time and Frequency Division
Boulder, Colorado, USA
Tel: 303-497-7674

Abstract— **As part of the accuracy evaluation of the NIST-7 primary frequency standard, we have investigated potential sources of frequency offsets due to the electronic servo system. We present results from investigations of RF spectral purity and synthesizer switching transients.**

I. Introduction

The Ramsey technique of separated oscillating fields is widely used in the field of atomic frequency standards. We have investigated potential sources of frequency shifts associated with the microwave radiation interrogating the atoms when using the Ramsey technique. We first measured the frequency bias that results from an interrogation signal whose spectrum contains imbalanced sidebands. We also investigated the frequency offsets that arise in determining the center of the Ramsey fringe using slow square-wave digital servos. These servos include a blanking interval to allow the atomic beam tube to reach steady state during the frequency modulation cycle. In addition to atomic beam transit time, there is an additional time delay that should be included in the servo's blanking interval. This delay is caused by anomolous switching transients in a direct digital frequency synthesizer.

II. RF Sideband Pulling

The presence of spurious, discrete sidebands in the spectrum of the microwave radiation can lead to errors in the determination of the center of the Ramsey peak. While these effects are not unique to slow square-wave digital frequency servos, they may be more pronounced in systems employing direct digital synthesis (DDS) due to phase accumulator truncation [1], and electromagnetic interference from high-speed digital electronics.

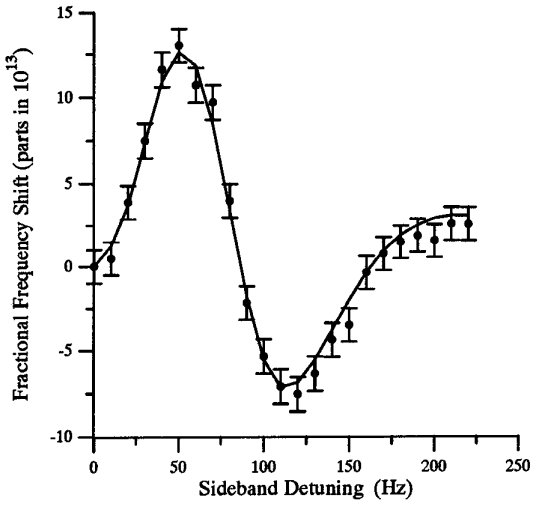

Fig. 1. Frequency Shift Due to Sideband Pulling. Solid line is the theoretical calculation. Dots are the experimental measurements. Carrier power: -2.5 dB relative to optimum power; lower sideband: -29 dBc; upper sideband: -66 dBc. Experiment duration: 300 s per point.

The frequency shift due to a discrete sideband has been calculated theoretically [2]. An independent calculation by one of us (J.H.S.) has confirmed that result, except that in their equation (9) the drift time T should be replaced by $T + \tau$, where τ is the transit time through one interaction region. For sideband detunings of the order of the Ramsey linewidth, we obtain shifts like those shown by the solid line in figure 1 when we average over the velocity distribution.

The calculations were verified experimentally using the United States primary frequency standard NIST-7 by intentionally modulating the microwave signal in both amplitude and phase to produce a well defined spectrum. The amplitude and phase of the carrier must be modulated coherently to yield imbalanced

sidebands. Consider the sum of three signals: a carrier, an amplitude modulated carrier, and a phase modulated carrier.

$$\begin{aligned} E(t) &= \mathrm{Re}\{Ae^{i\theta}e^{i\omega t} \\ &+ \beta Ae^{i\theta}e^{i\omega t}[1+\epsilon\cos(\Omega t+\phi)] \\ &+ \gamma Ae^{i\theta}e^{i\omega t}e^{i\eta\sin(\Omega t+\psi)}\} \end{aligned} \quad (1)$$

where A is the carrier wave amplitude, ω is the carrier frequency, θ is the carrier phase, ϵ is the amplitude modulation index ($\epsilon \leq 1$), Ω is both the amplitude and phase modulation frequency, ϕ is the phase of the amplitude modulation, η is the phase modulation index, and ψ is the phase of the phase modulation. β and γ are the relative amplitudes of the amplitude modulated and phase modulated signals with respect to the unmodulated carrier. If $\epsilon \ll 1$ and $\eta \ll 1$ this can be rewritten in three terms representing the carrier, the upper sideband and the lower sideband, respectively:

$$\begin{aligned} E(t) &= \mathrm{Re}\{(1+\beta+\gamma)Ae^{i\theta}e^{i\omega t} \\ &+ \frac{1}{2}Ae^{i\theta}(\epsilon\beta e^{i\phi}+\eta\gamma e^{i\psi})e^{i(\omega+\Omega)t} \\ &+ \frac{1}{2}Ae^{i\theta}(\epsilon\beta e^{-i\phi}-\eta\gamma e^{-i\psi})e^{i(\omega-\Omega)t}\}. \end{aligned} \quad (2)$$

The upper and lower sideband relative amplitudes can then be written

$$S_+ = \frac{1}{2(1+\beta+\gamma)}(\epsilon\beta e^{i\phi}+\eta\gamma e^{i\psi}), \quad (3)$$

$$S_- = \frac{1}{2(1+\beta+\gamma)}(\epsilon\beta e^{-i\phi}-\eta\gamma e^{-i\psi}). \quad (4)$$

If we choose $\epsilon\beta = \eta\gamma = \delta$, then the relative sideband intensities are

$$|S_+|^2 = \frac{\delta^2}{2(1+\beta+\gamma)^2}[1+\cos(\phi-\psi)], \quad (5)$$

$$|S_-|^2 = \frac{\delta^2}{2(1+\beta+\gamma)^2}[1-\cos(\phi-\psi)]. \quad (6)$$

The upper and lower sidebands have equal intensity for

$$(\phi-\psi) = \frac{\pi}{2} \pm n\pi, \text{ for } n = 0, \pm1, \pm2, \ldots. \quad (7)$$

To measure the frequency pulling with high accuracy and within a short time, we chose to introduce the maximum sideband asymmetry (a single sideband). This is achieved by setting

$$(\phi-\psi) = 0 \pm n\pi, \text{ for } n = 0, \pm1, \pm2, \ldots. \quad (8)$$

Such a single sideband modulator is realized with the circuit of figure 2. A low phase noise, 9-GHz microwave source (OSC-MAIN) is modulated in both amplitude and phase by two independent modulators of the type described in [3]. One modulator is optimized to produce high purity AM, while the other is optimized to generate only PM. Two phase-locked direct digital synthesizers ($\mathrm{DDS_{AM}}$ and $\mathrm{DDS_{PM}}$) provide the audio frequency modulation signals ($\cos(\Omega t+\phi)$ and $\sin(\Omega t+\psi)$) to two mixers. The synthesizers are adjusted (under computer control) so that $\epsilon\beta = \eta\gamma$ and $\phi = \psi + \pi$. This is verified by monitoring the microwave spectrum with a spectrum analyzer (FFT) at an intermediate frequency of 50 kHz, using a local oscillator (OSC-LO). The amplitudes of the carrier, lower, and upper sidebands are then recorded by the computer.

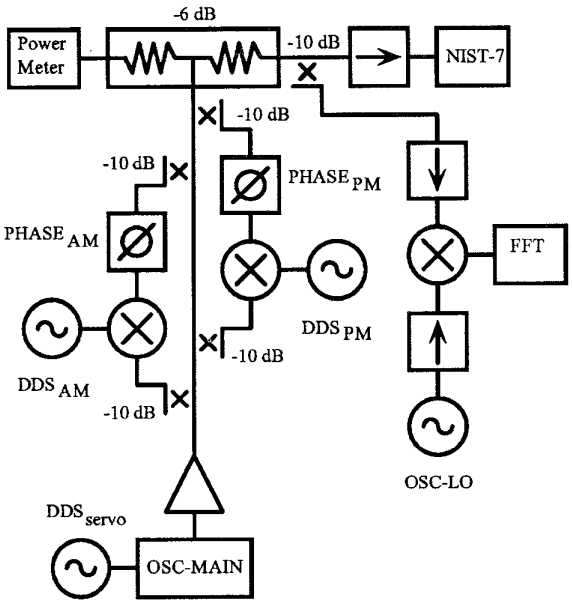

Fig. 2. Single Sideband Modulator.

The frequency bias introduced by this single sideband is determined by measuring the center of the Ramsey fringe using a slow square-wave frequency servo. The computer controlled synthesizer ($\mathrm{DDS_{SERVO}}$) modulates and steers the microwave source (OSC-MAIN). Figure 1 shows the measured frequency pulling (dots) as a function of the sideband detuning Ω. The error bars represent $\pm1\sigma$ statistical uncertainty. Since the experimental velocity distribution [4], sideband intensities, and detunings were used in calculating the theoretical curve, no free parameters were adjusted to obtain the agreement shown in figure 1. We have obtained similar results for detunings com-

parable to the width of the Rabi pedestal.

The theoretical curve in figure 1 is antisymmetric about zero detuning; hence symmetric sidebands produce shifts that cancel each other. Pure amplitude modulation generates symmetric sidebands about the carrier and does not lead to a frequency shift. Similarly, neither does pure phase modulation. This was verified experimentally by enabling only one branch of the single sideband modulator of figure 2 (either AM or PM) and measuring the center of the Ramsey fringe as a function of modulation frequency. Figure 3 shows that there is no significant frequency pulling for either amplitude modulation or phase modulation sidebands at -29 dBc.

The sideband pulling data of figure 1 can be used to calculate the frequency bias due to a pair of sidebands near the Ramsey fringe if the power dependence of the shift is known. The theory predicts that the shift is linear in sideband power. This was verified experimentally by measuring the center frequency of the Ramsey fringe as a function of sideband power. The results are shown in figure 4.

From these results, estimation of the frequency bias due to spurious RF sidebands can be made a routine part of the accuracy evaluation of a primary frequency standard.

III. Blanking Intervals in Slow Square Wave FM Servos

The use of direct digital synthesis in microwave synthesis chains has grown in recent years. This is due to improvements in the frequency resolution and agility of such synthesizers. Slow square-wave frequency servos are readily implemented when DDS instruments are computer controlled. The task of evaluating the frequency biases in such a servo is greatly simplified if the beam tube and electronics are allowed to reach steady state before the clock signal is measured. Thus, after a frequency step command is sent to the DDS, a blanking interval τ_b is established, during which the clock signal is discarded. After the blanking interval, the clock signal is recorded during the acquisition interval τ_a. It is desireable to have τ_a occupy a large fraction of the modulation period in order to enhance frequency stability. Simply reducing the modulation frequency is an unacceptable approach to increasing the ratio τ_a/τ_b, because it increases the system's sensitivity to noise that exhibits $1/f$ power spectra.

The blanking interval can be written as the sum

$$\tau_b = \tau_r + \tau_\phi + \tau_\rho, \qquad (9)$$

where τ_r (10 ms) is the response time of the DDS, that is, the time from the transmission of a frequency

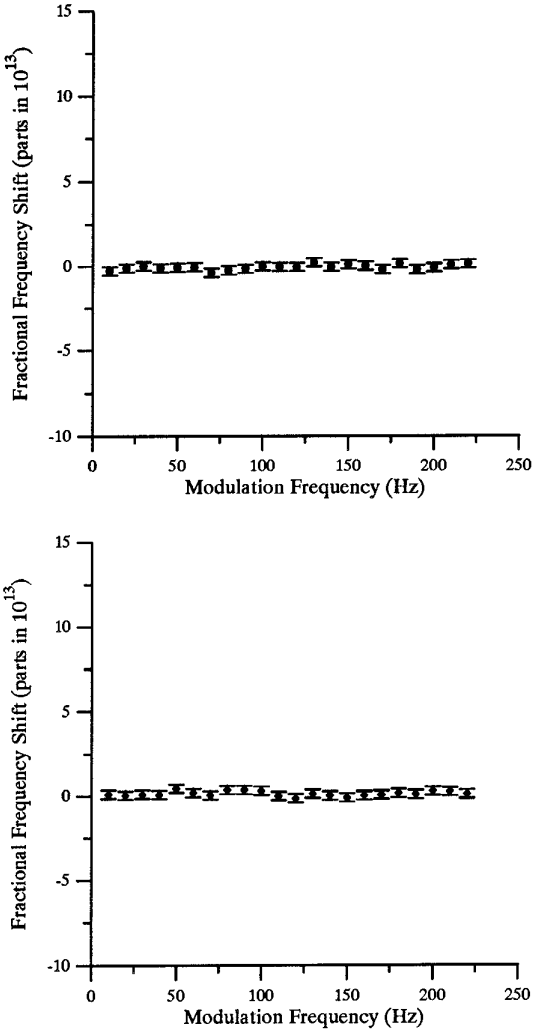

Fig. 3. Frequency Shift for Pure AM or PM
Upper Plot: frequency shift vs. amplitude modulation frequency. Lower Plot: frequency shift vs. phase modulation frequency. The modulation sidebands for both cases are -29 dBc. Experiment duration: 3000 s per point. For comparison, the horozontal and vertical scales are the same as figure 1.

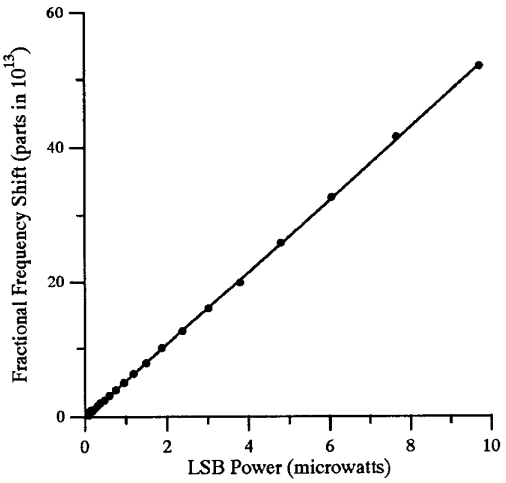

Fig. 4. Frequency Shift vs. Sideband Intensity
Dots are the experimental measurements. The 1σ uncertanties are equal to the symbol size. Carrier power: -2.5 dB relative to optimum power; sideband detuning: 50 Hz below carrier. Experiment duration: 1800 s per point. Solid line is a linear fit to the data.

step command to the change in frequency at the DDS output. τ_ϕ is phase-settling time of the DDS and τ_ρ (25 ms) is the transit time of the slowest atoms of interest across the Ramsey cavity and to the detection region. There is a lower limit placed on τ_b by τ_r and τ_ρ. We have, however, discovered techniques whereby τ_ϕ may be eliminated, improving frequency stability and eliminating a potential frequency bias.

IV. Synthesizer Switching Transients

We have found a potential frequency bias due to phase transients in a commercial direct digital synthesizer. The transients occur whenever the synthesizer is sent frequency control instructions by the computer. These transients are therefore synchronous with the frequency modulation, some occurring tens, and even hundreds of milliseconds after the frequency step is performed. Since the position of the Ramsey fringe is sensitive to the phase difference between the two ends of the cavity as seen by atoms taking several milliseconds to traverse the cavity, such phase transients can give rise to significant frequency offsets.

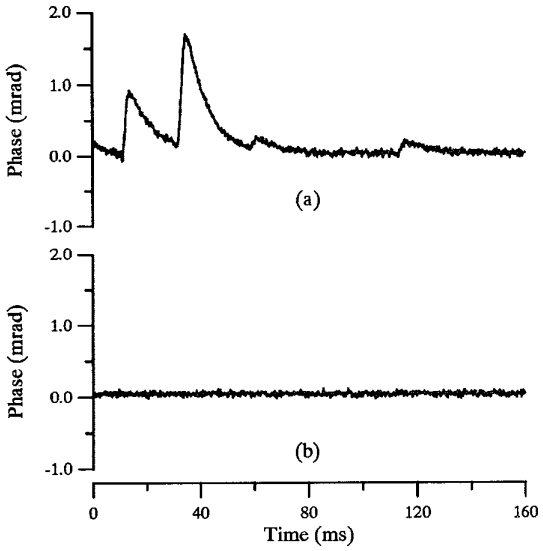

Fig. 5. Phase Transients Due to Computer Control.
Trace (a): phase transients occuring after frequency control command is sent to synthesizer at $t = 0$ ms. Trace (b): supression of phase transients when internal oscillator is bypassed.

The transients were measured by synchronously recording the relative phase of two synthesizers while one was sent frequency control commands by a computer. To simplify the measurement, the same frequency control command was sent to the synthesizer repeatedly, not changing the output frequency. Figure 5(a) shows the resulting phase transients. The peak phase deviation of 1.7 mrad occurs 35 ms after the instruction is sent to the synthesizer.

When a DDS unit is used in a microwave synthesis chain, it is common to provide the device with an external frequency reference. The DDS then phase-locks its own internal crystal oscillator to the external signal. We think that the "housekeeping" operations of the microprocessor within the DDS are inadvertently coupled to this phase-locked loop, generating phase transients that are synchronous with its operation. We were able to eliminate the phase transients by removing the instrument's internal crystal oscillator and instead injecting a suitable external reference frequency directly into the synthesizer's timing circuits. Figure 5(b) shows the dramatic improvement in phase stability.

Figure 6 shows the effect of the phase transient upon the atomic beam fluorescence as well as the normal

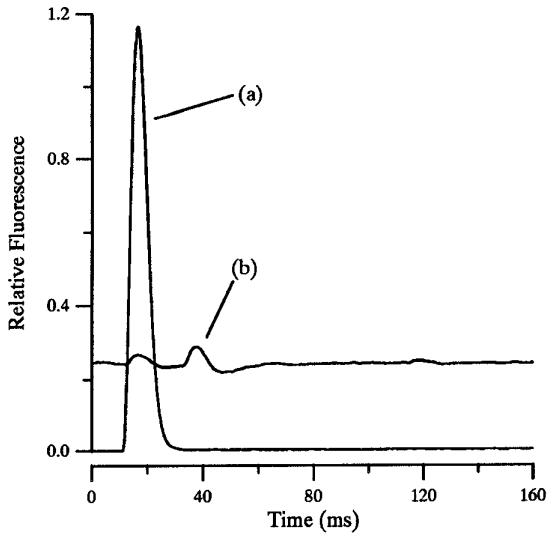

Fig. 6. Effect of Synthesizer Phase Transients. Trace (a): Normal slow square wave FM transient due to the atomic transit time distribution. This trace was taken with the frequency servo operating, thus the steady state fluorescence levels before and after the transient are equal. Trace (b): Effect of DDS phase transients (figure 5(a)) on atomic beam fluorescence with frequency fixed on the side of the Ramsey fringe. Trace (b) has been offset for clarity.

modulation transient. If we were to determine a blanking interval based solely upon the response time of the synthesizer and the atomic beam transit time distribution, the effect of the synthesizer switching transient would still introduce a significant contribution to the measured fluorescence.

The size of the frequency bias due to the switching transient was determined by measuring the center of the Ramsey fringe using two different direct digital synthesizers. Both units were identical except that one unit was modified to eliminate the phase transient. With a blanking interval of 40 ms, the fractional frequency bias produced by the transient was $(50 \pm 1) \cdot 10^{-13}$. Although the blanking interval might be extended to avoid the initial switching transients, periodic transients (visible in figure 5(a) at 120 ms) are virtually unavoidable.

We emphasize that these phase transients preserve their sign regardless of the sign of a frequency step performed by the DDS. Thus, the resulting bias cannot be eliminated through complex or pseudorandom modulation sequences. By removing these transients, we were able to transfer at least 20 ms from the blanking interval to the acquisition interval in each half of the modulation cycle.

V. Conclusion

We have investigated sources of bias in digitally controlled microwave synthesis chains: spurious RF sidebands and synthesizer switching transients. The experimental results obtained for RF sideband pulling are in excellent agreement with theory. They apply not only to digital servo systems but also to traditional analog servos. While the synthesizer switching transients we observed were unique to a specific model and might be avoided by selecting a different DDS, our modifications yielded a DDS with phase stability superior to other models we have tested.

References

[1] Nicholas, H. T., Samueli, H., "An Analysis of the Output Spectrum of Direct Digital Frequency Synthesizers in the Presence of Phase-Accumulator Truncation," 41st Annual Frequency Control Symposium, 1987, pp. 495-502.

[2] Audoin, C., Jardino, M., Cutler, L. S., and Lacey, R. F., "Frequency Offset Due to Spectral Impurities in Cesium-Beam Frequency Standards," IEEE Trans. Inst. Meas. vol. IM-27, 1978, pp. 325-329.

[3] Walls, F. L., "Extending the Range and Accuracy of Phase Noise Measurements," Proceedings of the 42nd Annual Frequency Control Symposium, 1988, pp. 432-441. U. S. Patent 4,968,908, "Method and apparatus for wide band phase modulation." (1990).

[4] Lee, W. D., Shirley, J. H., and Drullinger, R. E., "Velocity Distributions of Atomic Beams by Gated Optical Pumping," Proceedings of the 1994 IEEE International Frequency Control Symposium, pp. 658-661.